

(n,d) and (n,p) Reactions near $Z=50^*$

R. A. PECK, JR.

Brown University, Providence, Rhode Island

(Received March 10, 1961)

An emulsion study is reported of charged particles produced by 14-Mev neutron bombardment of Rh¹⁰³, In¹¹⁵, Sn¹¹⁶, Sn¹²⁰, Sb, and Te. For all but Te (no detectable yield) cross sections and spectra are presented, with distributions over the first 40° of laboratory angle of energy groups from Rh, In, and Sb. Contrary to an assumption common in earlier work, there is strong evidence that the (n,d) reaction contributes strongly. Five peaks among the Rh, In, and Sb spectra are identified with pickup transitions, the angular distributions conforming to Butler curves for uniquely predicted (2) or reasonable (3) l values. These values are consistent with target proton orbitals in all five cases. The wide (n,np) group is found at the expected energy in the Rh, In, Sn¹¹⁶ and Sb

spectra; its angular distribution is anomalous for Rh but displays the expected isotropy in the other three cases. Up to at least 6-Mev excitation the (n,p) gross structure is dominated by single-particle effects, the uncontaminated (n,p) yield obeying predictions of the Nilsson model as to spectral concentration and angular distribution; the low collective levels excited in (p,p') are not observed. Systematic behavior of the direct-interaction radius for (n,d) and (n,p) and of the reduced width for pickup are found to be reasonable. It is inferred that the parent state for proton pickup with low residual excitation is almost purely a single-particle state in the case of Sb, and has a strong single-particle character in Rh and a very weak one in In.

A MEASURE of the role of single-particle phenomena in reaction gross structure is the effectiveness of the orbital quantum number in determining angular distributions within the strength function resonances. This aspect of gross structure has not yet been examined in (n,p) reactions, nor has any aspect in the mass-100 region. The present survey of six nuclei was therefore undertaken as a study of (n,p) gross structure near a closed proton shell. Relative positions of groups found in the spectra are in reasonable agreement with those predicted from the Nilsson model, and were so interpreted in a preliminary report.¹

Further analysis has shown that these distributions are largely attributable to (n,d) reactions, the energy groups comprehending a small number of residual levels² and so being irrelevant to problems of gross structure. Analysis of the spectra and angular distributions of the principal groups from Rh, In, and Sb therefore leads, through a confirmation of the pickup forms expected (except for one new J^π assignment), to information on the systematic behavior of interaction radius and reduced width in the (n,d) process, not previously so studied for nuclei other than the lightest. Analysis of the proton contributions does admit some comparison with gross structure predictions at low excitation (up to about 6 Mev) and identification of the (n,np) contribution.

PROCEDURES

Ilford C2 plates (1 in.×3 in., 400 μ) were clamped with long edges parallel in a hollow square configuration. The 2-in. square projection of this array on the target plane, normal to all emulsions and 12.3 cm from the nearest end of each, enclosed the target, a 2-in. square

rolled foil in the cases of rhodium (33 mg/cm²), indium (64 mg/cm²), and the two tin isotopes (18 mg/cm²), and a circular evaporated deposit 1 in. in diameter (10 mg/cm²) in the case of antimony. The neutron source, a tritiated zirconium foil in a 170-keV Cockcroft-Walton deuteron accelerator, was situated 4.4 cm beyond the target plane and on the axis of the plate array. A brass chamber enclosing target and plates was evacuated for roughly twelve hours before exposures, in which between 0.6×10^{11} and 0.9×10^{11} neutrons were generated at the source in the various runs.

Track acceptance criteria were limited to surface origin and angle limits representing about twice the angular aperture of the actual target. An IBM 650 was used to compute for each track³ the target plane coordinates of the individual reaction site, angle between neutron and proton directions, proton's emulsion range and energy, and the reaction energy corrected for nuclear recoil. Tracks whose computed reaction sites did not fall inside the actual target boundaries by 5 mm or more were rejected. Since the data finally accepted are for 3000 tracks drawn from 11 000 measured, and since the directly measured data are thoroughly interwoven in the computed quantities, there is little likelihood of any residual observer bias. Nevertheless, all data sets (from different microscopists and/or plate areas) for each reaction were tested for consistency in the distributions over measured angle and dip and in the gross features of intensity, energy, and reaction angular distributions. Of 24 data sets, three were rejected at this screening and the rest are reasonably consistent in the respects noted. They provide between two and five independent data sets per reaction and show that computed target coordinates are accurate to 2–3 mm, corresponding to the expected accuracy (1°) of angle measurements, and that tracks are recorded with uniform efficiency up to the angle and dip limits imposed.

* Supported in part by the U. S. Atomic Energy Commission.
¹ *Proceedings of the International Conference on Nuclear Structure, Kingston*, edited by D. A. Bromley and E. W. Vogt (University of Toronto Press, Toronto, 1960), p. 783.

² From the three target nuclei providing most of the data, the (n,d) reaction forms an even product nucleus, and (n,p) an odd neutron product. Further, the residual excitation energy at a given emulsion range is several Mev less for deuterons than protons.

³ Corrections were applied to individual tracks for local variations in emulsion shrinkage, target thickness as a function of direction of travel, and neutron energy variation with target coordinates of the reaction site.

Total neutron exposures were determined accurately from volume proton recoil densities in the emulsions (2% consistency between observers) and checked against determinations from a Ra-Be-calibrated long counter (6% from emulsion value). For cross-section calculations the number of neutrons in the 14-Mev peak was used, 72% of the total number over 3 Mev as determined from the emulsion recoil spectrum. Background exposures identical to the rest except for removal of target materials from the thick gold and lead backings were normalized to total neutron exposures. Accuracy of this normalization is verified by the net yield reaching zero in several regions of the spectra but nowhere falling significantly below it.

The limit to energy resolution in emulsion measurements is set by accuracy of angle and dip measurements, the error inherent in range measurements being well below 1%. Since the full width of the 14-Mev peak in the emulsion recoil spectrum is 0.6 Mev, the intrinsic width being necessarily below 0.1 Mev, the width of an emulsion group corresponding to a sharp line in a reaction spectrum should be less than 0.5 Mev; the recoil spectrum is much more sensitive to errors in angular data than are any of the reaction spectra.

Since both detector and target dimensions are comparable to their separation, the ratio of observed angular distribution to the differential cross section is a reaction-angle-dependent efficiency function which is different for each data set. The function, a fourfold space integral of a transcendental integrand, cannot be expressed in closed form and was evaluated by an *ad hoc* program on the IBM 650. The typical form is of a mild forward peak falling to a plateau and thereafter to a fairly abrupt cutoff, and the range of significant recording was defined as that over which the efficiency function varied by less than a factor of two from the plateau value. This range included 0° in all cases and imposed an upper angular limit ranging from 40° to 60° for the various data sets.

Also required for absolute cross sections is the neutron flux at the target, which is known only through the total number of neutrons leaving the source. Inasmuch as the latter was a 1-in. diam circle, its size was comparable to its distance from the target, and the average flux at the target given by the integral over target coordinates of a flux function falling from near an infinite-source value at the center to the point-source function far from the center. The effect is a major one, since the infinite-source value of flux at the target, for a given total neutron production, is more than ten times the point-source value. The required function was estimated with the aid of two independent plausibility arguments, giving results differing by $\pm 8\%$ for the square targets and $\pm 4\%$ for the circular one. Uncertainty in this factor affects only absolute cross sections and values for antimony relative to the rest; it has no internal effect for any one reaction, nor among the first four.

RESULTS

The reaction spectra, with background removed, are displayed in Fig. 1 and angular distributions for those portions for which they are statistically significant in Fig. 2. Absolute cross sections are given in Table I together with details of assignments to be inferred from the angular distributions. A tellurium target was also analyzed, but no yield of statistical significance observed.

Experimental uncertainties affecting these data are of three types (1) Statistical probable errors are indicated by vertical bars in the figures and explicitly in the table. Only these affect relative points within the distributions or values within a column of Table I. (2) The systematic uncertainty affecting data for reactions relative to one another resides chiefly in the neutron exposure and is represented by probable errors in recoil density measurements ranging from 5% for Rh to 8% for Sn¹²⁰. (3) The finite source correction introduces a systematic uncertainty affecting all data of the first four reactions uniformly and having an independent uniform effect on all Sb data. Consistency figures of $\pm 8\%$ and $\pm 4\%$ for this factor have been noted; there is no reliable way to quantify an absolute uncertainty in it. Limits of error arising from effects overlooked may be estimated from the maximum variations among absolute cross sections derived from individual data sets for each reaction, viz., Rh $\pm 12\%$, In $+2\% - 35\%$, Sn¹¹⁶ $\pm 4\%$, Sn¹²⁰ $+7\% - 16\%$, Sb $\pm 25\%$.

Evidence for the assignment of much of the yield and most of the spectral structure to (n, d) reactions is discussed in the following sections but may be summarized beforehand for clarity. In the case of Rh + n, the groups observed have previously been reported by Colli *et al.*⁴ and identified as deuterons by discrimination of a dE/dx pulse. Agreement of their energies as determined from the scintillation and emulsion spectra is a firm identification of the particle type, since the two devices measure energy and range, respectively. Additional confirmation is the fact that the angular distributions of these groups are found to disagree with predictions for (n, p) but fit well with those for (n, d). The same situation applies to angular distributions of the In + n groups, which also display a marked homology⁵ to those of Rh(n, d). In Sb + n, the deuteron group is identified on the basis of an angular distribution favoring the (n, d) prediction. In all three cases the correspondence of groups with known levels of the (n, d) product is reasonable.

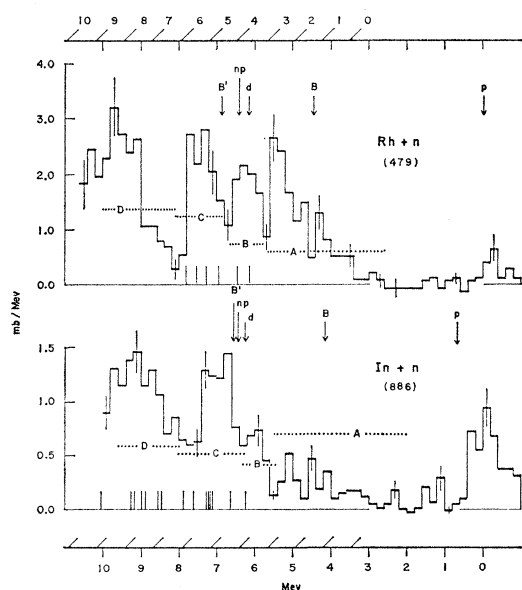
Spectra

The background spectrum⁶ is smooth except for a peak between 7 and 8 Mev on the proton scale of Fig. 1.

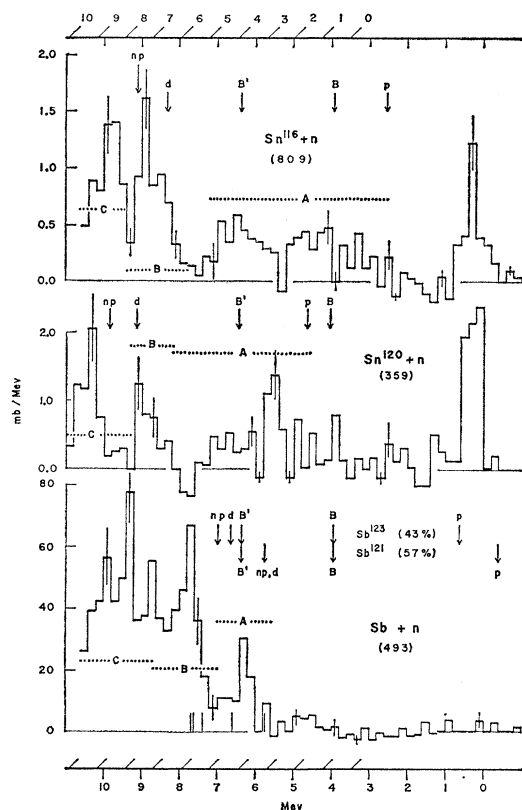
⁴ L. Colli, F. Cvelbar, S. Micheletti, and M. Pignatelli, *Nuovo cimento* 14, 1120 (1959).

⁵ The main structures of the Rh and In spectra are very nearly in line on the emulsion range scale, an accidental coincidence if different particles are involved. The (n, p) reactions differ in Q by 0.7 Mev, the (n, d) reactions by 0.0 Mev.

⁶ The ratio of net yield to background ranges from 8 to 24 in the rhodium and indium spectra, from 0.8 to 3 in the tin, and is above 5 in all parts of the antimony spectrum left of group A, for which it is 2.



(a)



(b)

FIG. 1. (a) and (b). Charged particle spectra from 14-Mev neutrons on indicated targets. *Ordinate*: Cross section integrated from 0° to cutoff (37° for Rh, In, Sn^{116} and 32° for Sn^{120} , Sb). Values are in mb/Mev of proton energy; multiply by 1.4 for mb/Mev of deuteron energy. Background has been subtracted, total (net) number of tracks in spectrum is shown in parentheses and statistical probable errors are shown. *Abscissa*: Proton scale (normal index marks, lower numerals) is exactly $U-Q$ and approximately E_n-E_p ; deuteron scale (oblique index marks and upper

This peak⁷ is visible in the gross yield from the tin isotopes only. Hydrogen contamination of rolled foils, including the gold backing and all targets except antimony, is apparent in concentrated groups appearing at $Q=0$ in the net spectra. Track analysis being based on the assumption that each track originates in the target foil, the position and concentration of the contamination group eliminates the possibility of assigning it to volume recoils in the emulsions. As expected, the hydrogen contamination group is absent only in the cases of the one evaporated target (antimony) and the one backing (lead) which was cleaned abrasively.

Vertical arrows in Fig. 1 indicate the positions of the highest energy groups from (n,p) , (n,d) , and (n,np) processes. First to appear (from the right) should be (n,p) , and while the maximum energy yield from (n,p) is too weak in these spectra to permit quantitative determination of Q values, it is a fact that in all five spectra the average net yield over several intervals first rises from zero approximately at the calculated energy.

Rhodium

The portion of the $\text{Rh}(n,d)$ spectrum previously identified by electronic discrimination⁴ consists of an incompletely resolved doublet occupying the first 2 Mev of excitation, followed by a gap 1-Mev wide and a higher group at least 2-Mev wide. These structures are well reproduced by groups B, C, and D in Fig. 1. The positions of B and C agree with those found by Colli *et al.* within 0.3 Mev. The energy of D is 0.9 Mev lower in Fig. 1 than in the scintillation spectrum, which may suggest a different mixture of particles in the two experiments, although the relatively large target thicknesses used in both experiments are most significant at the low energy of group D and may alone account for the discrepancy. Positions of these three groups disagree by 2 Mev or more if they represent protons. Only (n,p) and (n,d) can contribute to group B. Group C is energetically accessible to (n,np) but it has been shown⁸ that the characteristic maximum of that reaction occurs roughly 4 Mev below the maximum energy for intermediate nuclei, so that it is unlikely to contribute to group C. Group D is so situated that it could reasonably correspond to the (n,np) peak or the high-energy (n,d) group of Colli *et al.*; (n,t) and (n,α) are also energetically capable of contributing to it.

⁷ A similarly situated group has been reported [J. D. Seagrave, Phys. Rev. **97**, 757 (1955), Fig. 7] in the spectrum of recoil protons from a polyethylene radiator arising from degraded neutrons in the primary spectrum. Hydrogen contamination of targets and backing is noted in the text.

⁸ D. L. Allan, Nuclear Phys. **10**, 348 (1959); 6, 464 (1958).

numerals) is exactly E_n-E_d and approximately $U-Q$ (Q =reaction Q value, U =residual excitation). An exact (n,p) recoil correction has been applied in placing each track on the proton scale, and an average recoil term used to establish the deuteron scale. Arrows labeled p , d , and np indicate most energetic particles possible from (n,p) , (n,d) , and (n,np) , respectively. Protons and deuterons at the Coulomb barrier energy fall at B and B', respectively. Known levels in (n,d) product nuclei are shown by base line markings. Those for Sb apply to Sb^{121} as target; for Sb^{123} the ground and first excited states are shifted left by about 1 Mev.

FIG. 2. Angular distributions of energy groups. *Ordinate*: Differential cross section for central portion of group as labeled, about 1 Mev wide except for Rh A and In A which are taken 2 Mev wide. Units marked are 1 mb/sr for all Rh groups, 0.25 mb/sr for In, and 10 mb/sr for Sb. Statistical probable errors are shown. *Abscissa*: Cosine of reaction angle, in laboratory. *Curves* are Butler forms for assignments of Table I, the $l=4$ term being dotted in In C. Bg is background distribution from thick lead target.

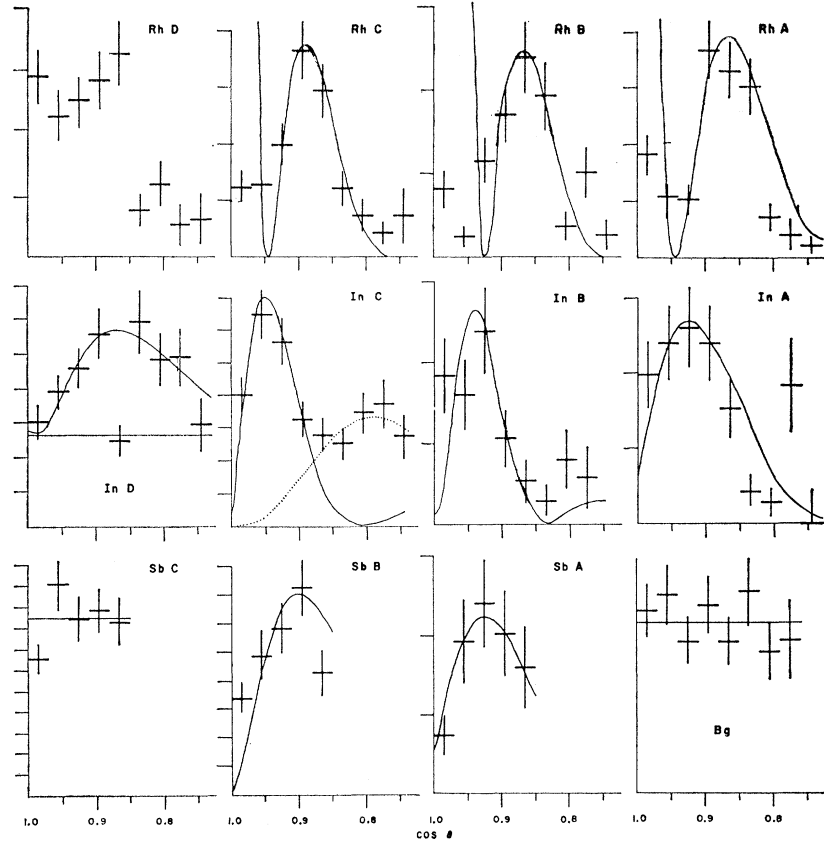


TABLE I. Summary of group data and assignments.^{18a}

Group	Energy range (Mev) ^a		σ (mb) ^b	Assignment in text ^c			
	(n,p)	(n,d)		Reaction	l_{\min}	r_0^d	width ^e
Rh D	8.1-10.0	2.6-5.2	3.6 ± 0.2	(n,p)(n,d) ^f			
Rh C	6.7-8.1	0.8-2.6	2.6 ± 0.2	(n,d) ^g	0	1.57	0.09
Rh B	5.7-6.7	-0.6-0.8	2.7 ± 0.2	(n,d) ^g	1	1.92	0.18
Rh A	2.6-5.7		3.0 ± 0.2	(n,p) ^h	0	2.10	
In D	7.3-8.9	2.4-4.5	2.5 ± 0.10	(n,p)(n,np) ^f	0	1.64	
In C	5.6-7.3	0.1-2.4	2.2 ± 0.15	(n,d) ^g	2	1.37	0.02
In B	4.8-5.6	-0.9-0.1	0.5 ± 0.05	(n,d) ^g	4	1.19	0.05
In A	1.3-4.8		0.7 ± 0.06	(n,p) ^h	2	1.80	0.03
Sn ¹¹⁶ C	6.9-8.1	1.4-3.1	0.9 ± 0.05^i	(n,np) ⁱ			
Sn ¹¹⁶ B	5.3-6.9	-0.7-1.4	1.4 ± 0.10	...k			
Sn ¹¹⁶ A	0.1-4.7		1.5 ± 0.07	...h			
Sn ¹²⁰ C	4.7-6.4	0.2-2.5	1.7 ± 0.14	...i			
Sn ¹²⁰ B	3.6-4.7		0.9 ± 0.09	...h			
Sn ¹²⁰ A	0.0-3.6		1.2 ± 0.10	...h			
Sb C ^k	9.2-11.0	4.1-6.6	86.3 ± 4.4^j	(n,np) ^f			
Sb B ^k	7.2-9.0	1.5-3.9	66.8 ± 4.5	(n,d) ^g	2	1.29	0.43
Sb A ^k	5.7-7.2	-0.5-1.5	18.5 ± 2.2	(n,p) ^h	3	2.20	

^a Excitation of residual nucleus corresponding to limits in Fig. 1.

^b Total cross section for group, extrapolated in angle to complete peak (Fig. 2). Statistical probable error is listed; see Results for systematic errors.

^c See Results for arguments.

^d See footnote 10.

^e Proton reduced width determined for (n,d) groups following Macfarlane and French. The quantity listed is $(C\theta)^2$, but C^2 is expected to be unity for proton pickup in intermediate nuclei (Reference 30, Appendix 1).

^f Accessible to (n,p), (n,d), (n,np), (n,t), and (n, α).

^g Accessible to (n,p) and (n,d) only.

^h Accessible to (n,p) only.

ⁱ Accessible also to (n,p), (n,d), and (n, α).

^j Isotropic group; differential cross section is given (mb/sr).

^k Excitation ranges given for Sb¹²³ target. For Sb¹²¹, (n,p) excitations are smaller by 1.0 Mev and (n,d) by 1.3 Mev.

Segment *A* of the rhodium spectrum is accessible only to the (n,p) reaction. It contains the suggestion of a group at the high excitation end but otherwise no evidence of structure. This portion of the spectrum cannot be compared with earlier work, since the only previous observation of this spectrum⁹ with energy resolution sufficient to show group structure is a scintillation determination, in which segment *A* is masked by the more intense deuteron groups lying to its left in the emulsion spectrum.

Indium

All of the foregoing remarks on the rhodium spectrum apply to the homologous and similarly labeled groups in that of indium, except that no published spectrum is available of sufficient resolution for comparison of structure. As in the case of rhodium, the indium groups are in quite reasonable agreement with the known levels in the (n,d) product nucleus.

Antimony

The isotopes of masses 121 and 123 are present in roughly equal quantities. As for rhodium and indium, the first few Mev of excitation in the (n,p) spectrum is strikingly weak. The first well-developed contribution (group *A*) is accessible to $\text{Sb}^{121}(n,d)$ but not $\text{Sb}^{123}(n,d)$; it is relatively weak, unlike the (n,d) ground state groups from Rh and In. There follows the energy gap which appears to be a systematic feature of Fig. 1, beyond which two or more strong groups appear. Group *B* is both too narrow and too energetic to fit the systematics of the (n,np) reaction and is probably to be assigned to (n,d) on the basis of its intensity, markedly greater than that of group *A*. Group *C* has the width and position appropriate to (n,np) , although it is energetically accessible to all reaction types mentioned in Table I.

Tin

The tin spectra show no convincing evidence of structure right of the position at which (n,np) is expected to appear. If, as in the other three spectra, the dominant process in that region is (n,d) , the residual level density is high and resolved contributions from separate levels not expected. The (n,d) reaction forms odd product nuclei from the tin isotopes and even ones from the other three targets.

Angular Distributions

No distributions are given for the tin isotopes because of their unfavorable signal:noise ratio.⁶ Those shown apply to restricted energy intervals removed by roughly 0.2 Mev, on the average, from the boundaries specified in Table I, to avoid confusion of adjacent segments. Neither the peaks which occur nor any differences in

their form can be instrumental in origin, for all groups in each spectrum have been weighted by the same energy-independent efficiency function and the purely geometric factors determining that function are the same for each reaction. The efficiency functions vary monotonically with angle and so do not introduce peaks. Finally, isotropic distributions do occur in some cases for which they are expected.

The angular distributions can be fitted to direct-interaction forms and the l_{\min} parameters identified if it is known what constitutes a reasonable value of the interaction radius.¹⁰ This information is not empirically available, since few direct interaction distributions have been published¹¹ and none for masses over 27. Variation of the (p,d) radius has been examined¹² up to mass 30, showing equal consistency with the conventional systematic expression, $1.7+1.2A^{1/3}$, and an empirical one, $4.37+0.42A$, for the nuclear radius. An isolated value of 1.29 has been found¹³ for (p,d) at mass 91. Extrapolation of the first empirical expression above to the mass range of this experiment suggests a probable (p,d) radius of 1.55 ± 0.1 ; extrapolation of the second empirical expression suggests an upper limit around 2.0, and a lower limit of 1.2 is estimated from the mass 91 value and the actual radius of the nuclear charge distribution.¹⁴ Since the (p,d) and (n,d) radii are the same among very light nuclei,¹¹ the same numbers may apply roughly to the (n,d) radius. For (n,p) the true interaction radius should lie between the charge radius (1.2) and the neutron density radius (1.75 ± 0.01 for these nuclei) deduced from nonelastic neutron cross sections.¹⁵ Wave function distortions should cause the true radius to lie below that deduced from Butler fits, for that is the sense of the effect of nuclear distortion alone and the two distortion effects appear to produce near cancellation in charge-symmetric reactions such as (p,p') .¹⁶ The difference between true and Butler radii may be guessed at by noting on the one hand that radii differ by 5%–20% for the groups of Fig. 2 as determined by fitting j_l^2 and $W^2(h_l, j_l)$, respectively, and on the other that radii determined from (p,p') distributions differ from the actual charge radius by 10%–20%. In summary, the (n,p) radius may be expected to fall near 1.8 and the (n,d)

¹⁰ All numerical values of radius mentioned in this paper designate $A^{-1/3}$ times the nuclear radius, in fermis.

¹¹ F. L. Ribe, Phys. Rev. **106**, 767 (1957); F. L. Ribe and J. D. Seagrave, *ibid.* **94**, 934 (1954); O. E. Overseth, Jr., and R. A. Peck, Jr., *ibid.*, **115**, 993 (1959).

¹² J. B. Reynolds and K. G. Standing, Phys. Rev. **101**, 158 (1956); E. F. Bennett, Princeton University Tech. Rept. NYO-8082, 1958 (unpublished).

¹³ C. D. Goodman and J. B. Ball, Phys. Rev. **118**, 1062 (1960).

¹⁴ R. Hofstadter, Revs. Modern Phys. **28**, 214 (1956).

¹⁵ J. H. Coon, E. R. Graves, and H. H. Barschall, Phys. Rev. **88**, 562 (1952). The neutron distribution in the nucleus serves to attenuate incident neutron flux without contributing to any (n,p) process.

¹⁶ S. T. Butler and O. H. Hittmair, *Nuclear Stripping Reactions* (John Wiley & Sons, Inc., New York); W. Tobocman and M. H. Kalos, Phys. Rev. **97**, 132 (1955); G. Schrank, P. C. Gugelot, and I. E. Dayton, *ibid.* **96**, 1156 (1954); R. G. Freemantle, D. J. Prowse, A. Hossain, and J. Rotblat, *ibid.* **96**, 1270 (1954).

⁹ L. Colli, U. Facchini, I. Iori, G. Marazzan, A. Sona, and M. Pignatelli, Nuovo cimento **7**, 400 (1958).

radius around 1.6, and both should surely lie in the range 1.2–2.4. Each radius should be the same for all nuclei studied, no magic-number irregularities having been found among these nuclei in the radii of either neutron or proton densities.

In analysis of the angular distributions, all l values of both parities from 0 to 5 have been considered for each group, and both (n, p) and (n, d) reactions. An l term is considered to give a possible fit if the required radius lies in the range 1.2–2.4 and the corresponding curve passes within the horizontal bars of the data in Fig. 2 at half maximum. The latter conditions permits a range of 0.03 in the cosine of the reaction angle and requires agreement of full width at half maximum within roughly 10° . A “best fit” is one most closely reproducing the observed peak width with a radius in the range imposed. Theoretical curves used are of the full Butler-Born approximation form.^{17,18}

(n, d) groups^{18a}

Groups *B* and *C* from rhodium, if proton groups, can be fit only by $l=0$, which is in flat disagreement with the single-particle orbitals available to contribute to the gross structure¹⁹; they have, further, been established as deuteron groups as discussed earlier. Rh *B* spans two residual levels, at 0 Mev ($0+$) and 0.475 Mev ($2+$), both contributing $l=1$ which fits the observed peak (radius 1.92). Rh *C* extends over three levels, at 1.57 Mev ($2+, l=1$), 1.88 Mev (J^π unknown), and 2.26 Mev ($2-$ or $3-, l=2$) of which the last is unlikely on energetic grounds to contribute. The best fit to the distribution is for $l=0$, radius 1.57, so that the principal contributor is presumably the 1.88-Mev level with parameters $0-$ or $1-$. Group *B* of indium can only represent the (n, d) product ground state ($0+$) which contributes the term $l=4$, one of the two terms ($l=4$, radius 1.80; $l=3$, radius 1.30) which best fit the data. Group *C* of indium covers four product levels, ranging from 1.21 to 1.37 Mev ($0+, 2+, 4+$), expected to contribute $l=0, 2$, and 4 . The best fit to the principal peak is for $l=2$ (radius 1.37), and the second maximum, if real, represents $l=4$ (radius 1.19, dotted curve in Fig. 2). Group *B* of antimony is best fit as a deuteron group with $l=2$ (radius 1.29), the only alternative being $l=3$ (radius 1.88). If due to Sb^{121} , it spans product levels at 2.22 Mev ($4+, l=2$), 2.42 Mev ($6+, l=4$) and 2.51 Mev ($7-, l=5$); if due to Sb^{123} it includes only a level at 1.14 Mev ($2+, l=2$). From either isotope, the expected contribution agrees with the empirical best fit.

¹⁷ S. T. Butler, Phys. Rev. **106**, 272 (1957).

¹⁸ C. R. Lubitz, H. M. Randall Laboratory of Physics, University of Michigan, Ann Arbor, 1957 (unpublished).

^{18a} See Appendix added in proof.

¹⁹ Features of (n, p) gross structure predicted for distorted nuclei of intermediate mass by the Nilsson model have been submitted to Nuclear Physics.

(n, p) distributions

The spectral range *A* from both rhodium and indium is energetically available only to the (n, p) reaction, and in both cases the angular distribution has the sharp peak expected of gross structure dominated by direct interaction. In the case of rhodium, for which the net yield is sufficient to permit angular distributions of subdivisions of the range, the same distribution is found for the high- and low-energy parts. For rhodium only one fit is possible, to $l=0$ (radius 2.10). This term is predicted in the (n, p) gross structure but with intensity only 20%–30% as great as that of other predicted contributions not observed. It is reasonable, of course, that the restricted angular range studied in this experiment should select a minority component. For indium also, only one fit is possible: to $l=2$ (radius 1.79). In this case the values 1 and 2 are predicted with equal intensity if the source proton is the unpaired one, and $l=2$ predominates if other protons in the valence shell contribute.

Attributed to Sb^{123} , group *A* of antimony can only be an (n, p) group and no fit is possible. It could contain contributions from $\text{Sb}^{121}(n, np)$ but is energetically unlikely to be dominated by them. The best fit would be for an $\text{Sb}^{121}(n, d)$ group with $l=3$ (radius 1.79), but the residual levels available under this interpretation are only those at 0 Mev ($0+, l=2$) and 1.18 Mev ($2+, l=0$); neither of the latter is a possible fit to the data. The group must therefore be attributed to $\text{Sb}^{121}(n, p)$, for which the best fit is to $l=3$ (radius 2.20), agreeing with the predicted gross structure providing the proton comes from the filled shell. This is not unreasonable at the excitation involved, and provides a simple account of the fact that the intensity of group *A*, while not strong, is markedly greater than (n, p) intensity at lower excitation. Many more source protons are available in the filled shell, of course, than in the valence shell.

(n, np) groups

Groups *D* from rhodium and indium and *C* from tin-116 and antimony are all properly situated to represent the (n, np) maximum and, as is appropriate to that process, clearly are or could be perceptibly wider than other groups. From antimony and tin-116, isotropic angular distributions confirm this identification. In indium group *D*, a large isotropic component appears together with a broad peak, suggesting either (n, p) or (n, d) in combination with (n, np) . The only possible fit to the peak for (n, d) is to $l=3$ (radius 1.82), and all the known parities of (n, d) product levels in the relevant excitation range are positive, requiring even l values. Since all the parities are not known, however, the possibility of (n, d) in this group cannot be ruled out. For an (n, p) group the best fit is to $l=0$ (radius 1.64), and in the (n, p) gross structure contributions are strong from single-particle levels of the seventh oscillator shell, leading to high-intensity predictions of $l=0, 1, 2$, and 3 . The

most probable assignment of group *D* of indium, therefore, is to a mixture of (n, np) and (n, p) with $l=0$.

Group *D* of rhodium should, on energetic grounds, contain a strong (n, np) component. Its peculiar angular distribution, however, is not isotropic and cannot be matched by any reasonable combination of direct-interaction forms. If correct, the shape would be suggestive of interference between l terms (reference 17, p. 282). A coincidence of positive and negative fluctuations in successive angular cells is more likely, the true distribution being a single broad peak with little or no isotropic background. In this case, the group would appear to represent $l=2$ for either protons or deuterons, neither of which would be inconsistent with available information since the (n, d) product level scheme is incomplete and $l=2$ is among the four terms predicted in the (n, p) gross structure. In view of the coincidence in energy of this group with an (n, d) group identified by scintillation spectrometry,⁴ it is very likely that (n, d) is present, but, since the cross section here found is substantially larger than the scintillation value, a second component is also indicated. Whether the second component is anisotropic (n, np) yield or (n, p) gross structure with (n, np) being anomalously suppressed cannot be determined from the data.

Cross Sections

Most extensive data available for comparison with the absolute cross sections of this experiment are for $Rh+n$. One of the four published studies is an emulsion determination²⁰ and so directly comparable regardless of relative contributions of protons and deuterons. The total cross section found here (groups *A*, *B*, and *C*, $1 \geq \cos\theta \geq 0.8$) is within 3% of the corresponding value of Brown *et al.* The same cross section determined by scintillation spectrometry²¹ is 44% smaller, and the forward differential cross section (average over $1 \geq \cos\theta \geq 0.97$), also determined by the scintillation method,²² 25% smaller than the result of this experiment. The quoted uncertainties in the latter two values are 27% and 10%, respectively, so the discrepancies need not be significant.²³ If they are, a systematic overestimate in the emulsion values, for which the normalization of background is checked by vanishing of net yield in some portions of the spectra, is less likely than the alternative of some loss of legitimate yield in gating a scintillation spectrometer by a dE/dx pulse. Finally, the scintillation determination⁴ of the absolute cross section contained in groups *B*, *C*, and *D* is 73% lower than that found

here. This is qualitatively consistent with the reaction assignments of Table I but again suggests some loss of particles in the counter telescope.

For indium, the forward differential cross section found by Eubank *et al.*²² is 1.6 ± 0.3 mb/sr, while this experiment gives 1.9–2.7 mb/sr depending on how much of group *D* is included. Again the combined experimental uncertainties exceed the discrepancy, but again the scintillation value is the lower. Data of Verbinski *et al.*²¹ for indium comprise all laboratory angles and cannot be adjusted to the angular range of this experiment since the distribution is not shown. In a gross sense the two experiments are not inconsistent; the counter determination is 20 ± 9 mb for all angles, to be compared with 3.4 mb in the small-angle peak of this experiment. In an emulsion study, Allan has set an upper limit of 1.1 mb/sr to the $In+n$ differential cross section at 120° and hence, presumably, to the genuinely isotropic component, for an energy range which appears to include only group *D* of this experiment.²⁴ The minimum differential cross section here found at small angles for group *D* is 0.6 mb/sr.

For the forward differential cross section of natural tin, Eubank *et al.*²² have assigned an upper limit of 1 mb/sr, while in this experiment the average over 0° – 40° is 1.8 ± 0.6 and 2.4 ± 0.6 mb/sr, respectively, for the isotopes 116 and 120; the uncertainties quoted reflect ambiguity in the low-energy cutoff corresponding to the scintillation spectrum. If the tin angular distributions peak beyond 0° as do most of the groups in Fig. 2, the agreement is good. For the energy range corresponding to Allan's upper limit²⁴ of 0.4 mb/sr at 120° , also for natural tin, the minimum differential cross section here found at small angles appears to be about 1 mb/sr for each isotope. In view of the statistical poverty of the angular distributions for tin, this discrepancy is not significant.

For natural antimony Eubank *et al.*²² report a forward differential cross section of 40 ± 2 mb/sr over an energy range apparently including groups *A* and *B*. The comparable value from this experiment is 45 ± 5 mb/sr, the uncertainty again referring to the appropriate low-energy cutoff. Allan's value²⁴ for the differential cross section at 120° is 0.9 ± 0.5 mb/sr, which is nearly two orders of magnitude smaller than the minimum values found in this experiment at small angles. This gives further support to the proposition previously advanced^{22,24,25} that the antimony spectrum at small angles is very strongly dominated by direct interaction events.

The failure to record any significant yield from $Te+n$ duplicates the experience of Eubank *et al.*²²

²⁰ G. Brown, G. C. Morrison, H. Muirhead, and W. T. Morton, *Phil. Mag.* **2**, 785 (1957).

²¹ V. V. Verbinski, T. Hurliman, W. E. Stephens, and E. J. Winhold, *Phys. Rev.* **108**, 779 (1957).

²² H. P. Eubank, R. A. Peck, and M. R. Zatzick, *Nuclear Phys.* **10**, 418 (1959).

²³ Comparisons are sensitive to the low-energy cutoff; exact agreement could be achieved in both cases by inclusion of an *ad hoc* fraction of group *D*.

²⁴ D. L. Allan (to be published); see also reference 1, p. 838. Corrections applied for unexamined high-energy yield may have restored some of the content of groups *A*, *B*, and *C*, though not any direct interaction contributions.

²⁵ R. A. Peck, H. P. Eubank, and R. M. Howard, *Nuovo cimento* **14**, 397 (1959).

DISCUSSION

For the tin isotopes and tellurium, the (n, d) process transforms an even-even nucleus into an odd-proton type, and (n, p) an even-even nucleus into an odd-odd one. For tin, the breaking of an unusually strong proton bond is also entailed in either event. It is not surprising that these reactions exhibit small cross sections, as found, as well as low Q values.

It seems clear that (n, d) offers strong competition to (n, p) and (n, np) in indiscriminated spectra, especially those from scintillation spectrometers. Consequently, most (n, p) distributions and cross sections (other than activation values) now in the literature must be suspected of (n, d) contamination. The effect is accentuated by the tendency of (n, d) to appear strongly at low residual excitation, in extreme contrast to (n, p). Proton pickup rather than knockout seems to contribute the dramatically large (n, x) cross section for antimony.²²

Two features of these data which are unexpected, though not in conflict with any known facts, are: (1) the apparent contribution of (n, p) rather than (n, d) to group *D* of indium and (2) the probable absence of (n, np) from, and the peculiar angular distribution of, group *D* or rhodium.

Whether identified from known level parameters or by a unique fit in the "reasonable" range of radii, each Butler curve in Fig. 2 defines an interaction radius¹⁰ quite narrowly. Several systematic features of interest arise from comparison of those values. The interaction radius rises with the emergent particle energy, as usual. It is consistently larger for (n, p) than for (n, d). This suggests that a closer approach of the neutron, and hence a stronger overlap of its wave function with the target proton's, is required for capture than for scattering, which is reasonable. The radius is in all cases larger for rhodium than for indium. This also is reasonable, since the proton wave functions in nuclei immediately preceding magic numbers may be expected to be more tightly concentrated than in more normal ones, requiring closer approach for a given degree of wave function overlap in the former than in the latter case.

(n, p) Reactions

It is found that the angular distributions of the direct interaction form persist in the (n, p) process at least up to roughly 6 Mev excitation, a fact already noted⁸ for lighter nuclei, which gives qualitative evidence of the importance of single-particle processes in forming (n, p) gross structure. All (n, p) angular distributions identified are consistent with forms expected in the gross structure, but the multiplicity of predicted terms resulting from deformation of the nuclei involved robs this consistency of force. A further correspondence is the fact that (n, p) yield first appears in strength at excitations corresponding to the beginning of single-particle levels of the sixth oscillator shell in the product nucleus.^{1,26} The strong dip

occurring at around 7–8 Mev in the rhodium, indium, and antimony spectra coincides in each case with the gap between single-particle level concentrations of the sixth and seventh oscillator shells, but is also consistent with known level patterns in the (n, d) product nuclei.

One argument for a collective interpretation of the persistent low-excitation gross structure excited by inelastic proton scattering rests on the fact that it does not appear in (p, n) and (n, p) spectra.²⁷ It is therefore of interest to note its absence from these (n, p) reactions. The implication is not entirely clear, however, for (n, p) also fails to excite a low-lying gross structure strongly excited by (d, p) in these nuclei.^{26,28} This is clearly not an instrumental effect, for scintillation spectrometer studies confirm the weakness of (n, p) yield at low excitation, while in the experiment reported here high-energy protons emanating from target hydrogen are recorded with good intensity.

(n, d) Reactions^{18a}

Two of the five (n, d) assignments of Fig. 2 and Table I fit unique predictions, two fit single predictions from a number, and one, in the absence of complete level information, affords a new assignment. Finally, we may note a consistent pattern among the reduced widths to which these fits correspond (Table I).

The listed values for group *B* of rhodium and for the $l=4$ component²⁹ of group *C* of indium are presumably high because, in each case, two levels are supposed (in the assignments made) to contribute the same l term. If compensation is made for these cases of multiple contribution, we find reduced widths per level of about 0.03 for all three cases in indium, 0.1 for both in rhodium, and 0.4 for antimony.

We expect that, antimony containing one proton beyond the closed shell and indium one proton under, the antimony ground state should have the strongest single-particle character and indium the weakest of the three. This corresponds exactly to the numerical sequence above. The reduced width per level is roughly constant within each reaction. The very large cross-section ratio of group *B* of antimony to the corresponding group of rhodium is reduced fivefold when translated into a ratio of reduced widths per level; the reduction is ninefold (and again toward unity) when antimony is compared with indium. These facts support the essential validity of the method³⁰ of extracting reduced widths.

Single-particle reduced widths extracted from (d, p)

²⁷ B. L. Cohen, Phys. Rev. **116**, 426 (1959). See also reference 1, p. 310 ff.

²⁸ B. L. Cohen, J. B. Mead, R. E. Price, K. S. Quisenberry, and C. Martz, Phys. Rev. **118**, 499 (1960).

²⁹ Of the ratio of the reduced widths for the two components of this group, one factor of 1.5 is a genuine cross section difference and another is associated with the different radii required to fit the two maxima. It is unlikely that the radius is really different for the two l terms, so the latter factor may probably be attributed to (a difference in) the error inherent in reduced width extracted by Butler-Born approximation.

³⁰ A. H. Macfarlane and J. B. French, Revs. Modern Phys. **32**, 567 (1960).

²⁶ R. A. Peck, Jr., and J. Lowe, Phys. Rev. **114**, 847 (1959).

and (p,d) data for the states relevant to these nuclei are of order 0.02–0.03, corresponding to 0.3–0.4 as computed from square-well eigenfunctions.³¹ If the single-particle widths to be obtained from Butler-Born approximation analysis of (n,d) are likewise assumed to be tenfold smaller than the square-well values, the experimental numbers mentioned one paragraph above imply experimental error factors of five and more. Since such errors are inconsistent with the most pessimistic accumulation of experimental uncertainties, the alternative conclusions seem to be established, *viz.*, that (1) single-particle widths corresponding to experimental reduced widths extracted from these (n,d) distributions by the Butler-Born approximation method are of the same order as those computed from simple eigenfunctions, and (2) the pickup reduced width for antimony is about the same as the single-particle width, that for rhodium less but comparable, and that for indium very much less than the single-particle width.

APPENDIX (added in proof)

Alternative Assignments for (n,d) Groups

The assignments (Table I) discussed in the text rested on observed peak widths and an estimated range of reasonable magnitudes for radius; groups were not compared in making the assignments, on the principle that distortion effect systematics is unknown for the (n,d) process. An alternative guide is the consideration that the radius, regardless of its apparent magnitude, should be sensibly constant over the ranges in excitation and mass covered by the five (n,d) groups. A unique radius is defined by the latter assumption alone, the corresponding assignments differing from those of Table I for three of the five groups. These assignments appear in Table II together with the resulting final-state spin and parity, radius parameter and reduced width.

In Table II the radii vary within $\pm 5\%$ rather than $\pm 20\%$ as before, and the (n,d) radius comes much closer to that for the (n,p) groups. The quality of fit is less uniform than before over the set of five distribu-

tions, but follows a reasonably systematic pattern. The low excitation group (B) gives a Butler curve narrower than the observed peak by 31%, 13%, and 22% for Rh, In, and Sb, respectively, and the higher excitation group (C) a Butler curve wider than the experimental one by 43% and 1% for Rh and In.

Populated proton states in the unfilled target shell are $1g_{9/2}$, $1f_{5/2}$ and both $2p$ states. The unpaired proton appears to dominate the low-excitation group, as expected, for both Rh and In reactions. It is difficult to understand why f protons should predominate over p in In C, but it should be noted that the angular distribution of this group has a weakly indicated secondary peak which could represent the expected $l=1$ component. While a radius parameter of 1.5 is required to fit $l=1$ to the small peak position, the poor definition of the latter and the strong contribution from $l=3$ preclude quantitative arguments. The strong contribution of g protons to Rh C is quite reasonable. As for Sb B, while strong contributions from the p, f, g shell are to be expected since there is only one valence proton, it is not clear why f protons should predominate.

Final spins and parities are definitely known for levels occurring within the groups Rh B and In B, and agree with Table II (for Rh B, $0+$ at 0.00 Mev and $2+$ at 0.48 Mev; for In B, $0+$ at 0.00 Mev). The fact that the prediction of l_{\min} is unique for each of these groups and agrees with the observation establishes the uniform radius of Table II as the correct one. In the excitation span of Sb B a level is known which fits the assignment from this group ($7-$ at 2.51 Mev in Sn¹²⁰). In the excitation ranges of the two C groups are no known levels of the required spins and parities, although Rh C could be due to a level whose parameters have not been measured (1.88 Mev in Ru¹⁰²). It is not necessarily to be expected, however, that the (n,d) product levels for these nuclei should be known from previous work. Knowledge of these level schemes derives from β^+ -decay gammas, (d,p) and (α,α') reactions, none of which is very likely to excite the hole states generated by proton pickup. The (n,d) levels should be visible in (d,He^3) spectra, but none have been published for these nuclei.

The systematic pattern of reduced widths is not changed by the new assignments. Neither the widths of Table II nor those of Table I are proportional to the populations of the single proton states in the target nuclei. For either set of assignments the two values of width per level for In are essentially the same, as are the two for Rh. The pattern $\theta_{Sb}^2 \gg \theta_{Rh}^2 \gg \theta_{In}^2$ applies in either case.

I am indebted to B. J. Raz for the suggestions and discussion incorporated in this Appendix.

TABLE II. (n,d) group assignments for constant radius.

Group	l_{\min}	J_{final}^*	r_0	width
Rh C	4	5,6—	2.00	0.07
Rh B	1	0,1,2,3+	1.92	0.18
In C	3	0,1—	1.93	0.02
In B	4	0+	1.80	0.03
Sb B	3	6,7—	1.88 ^a	0.34

^a Assuming Sb¹²¹ as target isotope; 0,7,8— for Sb¹²³.

³¹ Reference 30, Fig. 60 and Eqs. VII. 6, 7.